

A Well-balanced Finite Volume Scheme for Shallow Water Equations with Porosity - N°22

Minh H. Le¹, Virgile Dubos³, Marina Oukacine¹ and Nicole Goutal^{1 2}

¹Saint-Venant Hydraulics Laboratory (LHSV), ²Electricity of France (EDF) R&D, Chatou, ³Sorbonne University, Inria, LJLL, ANGE

Framework

- ▶ Modelling emergent and rigid vegetation in open-channel with a single porosity-based shallow water model (SP) [1].
- ▶ New Godunov-type, finite volume, well-balanced and shock capturing scheme for SP.
- ▶ Comparison with other methods in the literature [2, 3] and first application.

Single porosity shallow water model

$$\partial_t W + \partial_x F + \partial_y G = S_b + S_\phi + S_\tau \quad (1)$$

$$\text{with } W = \phi \begin{pmatrix} h \\ hu \\ hv \end{pmatrix}, F = \phi \begin{pmatrix} hu \\ hu^2 + \frac{g}{2}h^2 \\ huv \end{pmatrix}, G = \phi \begin{pmatrix} hv \\ huv \\ hv^2 + \frac{g}{2}h^2 \end{pmatrix},$$

$$S_b = \phi \begin{pmatrix} 0 \\ -gh\partial_x b \\ -gh\partial_y b \end{pmatrix}, S_\phi = \begin{pmatrix} 0 \\ \frac{g}{2}h^2\partial_x \phi \\ \frac{g}{2}h^2\partial_y \phi \end{pmatrix}, S_\tau = - \begin{pmatrix} 0 \\ g\phi h \frac{\eta^2 |U|}{h^{4/3}} u + \frac{1}{2} \frac{a C_d h |U|}{\phi} u \\ g\phi h \frac{\eta^2 |U|}{h^{4/3}} v + \frac{1}{2} \frac{a C_d h |U|}{\phi} v \end{pmatrix}.$$

where

$$\begin{cases} h : & \text{depth of water,} \\ b : & \text{bed elevation,} \\ \eta : & \text{Manning's coefficient,} \\ C_d : & \text{drag coefficient,} \\ \phi : & \text{porosity,} \end{cases} \quad \begin{cases} u, v : & \text{depth-averaged horizontal velocities,} \\ g : & \text{acceleration due to gravity,} \\ D : & \text{effective diameter of vegetation,} \\ a = \frac{1-\phi}{\pi D/4} : & \text{frontal area of vegetation.} \end{cases}$$

Numerical scheme

Well-balanced scheme : we solve (1) in two following steps:

$$\begin{cases} \text{Convection:} \\ \partial_t W + \partial_x F + \partial_y G = S_b + S_\phi, \\ W(x, 0) = W^n. \end{cases} \quad (2) \quad \begin{cases} \text{Friction and Drag:} \\ \partial_t W = S_\tau, \\ W(x, 0) = W^{n+1/2}. \end{cases} \quad (3)$$

$$\text{FV scheme for (2): } W_j^{n+1/2} = W_j^n - \frac{\Delta t}{|C_j|} \sum_{\Gamma_{jk} \subset \partial C_j} |\Gamma_{jk}| \mathcal{F}(W_j^n, W_k^n; b_j, b_k).$$

Rotational invariance of the flux \Rightarrow numerical flux derived from the 1D system (4).

$$\begin{cases} \partial_t W + \partial_x F = S_x, \\ W(x, 0) = \begin{cases} W_L & \text{if } x < 0, \\ W_R & \text{if } x > 0. \end{cases} \end{cases} \quad (4) \quad \text{Riemann } (\mathcal{R}_.) \text{ problem with } S_x(W, b) = (0, \frac{g}{2}h^2\partial_x \phi - g\phi h\partial_x b, 0) \text{ and } W_{L,R} \text{ the projected states } W_{j,k}^n \text{ on } \Gamma_{jk}.$$

Approximation by simple-solver $W_{\mathcal{R}}(x/t)$ of (4):

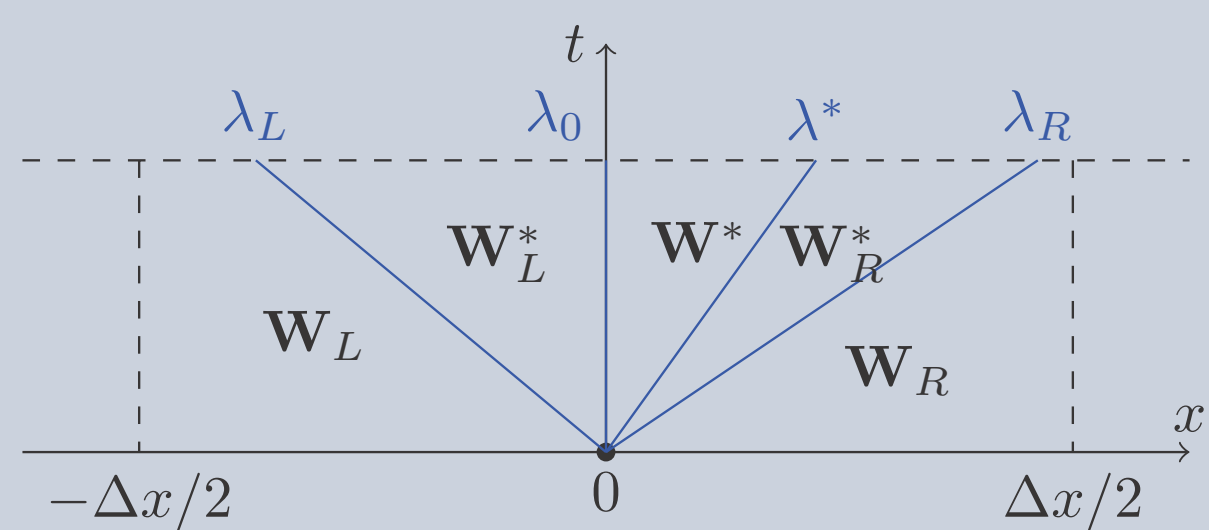


Figure: Four-wave approximate solution of (4).

Determination of intermediate states:

- integral consistency condition:

$$\frac{1}{\Delta x} \int_{-\frac{\Delta x}{2}}^{\frac{\Delta x}{2}} W_{\mathcal{R}} \left(\frac{x}{\Delta t} \right) dx = \frac{1}{\Delta x} \int_{-\frac{\Delta x}{2}}^{\frac{\Delta x}{2}} W \left(\frac{x}{\Delta t} \right) dx \quad (5)$$

- HLL state for homogeneous $\mathcal{R}_.$ problem:

$$W^{HLL} = \frac{\lambda_R W_R - \lambda_L W_L}{\lambda_R - \lambda_L} - \frac{F(W_R) - F(W_L)}{\lambda_R - \lambda_L}$$

- $\mathcal{R}_.$ invariants across contact discontinuities:

$$\phi hu = \text{cst.}, u^2/(2g) + h + b = \text{cst.}, v = \text{cst.} \quad (6)$$

- (5) and 1st invariant in (6) lead to:

$$(\phi h)^{HLL} = \alpha \phi_R h_R^* + (1 - \alpha) \phi_L h_L^*, \quad \alpha = \frac{\lambda_R}{\lambda_R - \lambda_L}, \quad (7)$$

$$(\phi hu)^{HLL} = q^* - \frac{\Delta x \bar{S}_x}{\lambda_R - \lambda_L}, \quad \bar{S}_x = \frac{1}{|C|} \int_C S_x dx dt. \quad (8)$$

First order Godunov-type scheme :

$$W_j^{n+1/2} = W_j^n - \frac{\Delta t}{\Delta x} (F_{j+1/2}^L - F_{j-1/2}^R)$$

$$\begin{cases} F^L = F(W_L) + \lambda_L (W_L^* - W_L) + \lambda^* (W^* - W_L^*), \\ F^R = F(W_R) - \lambda_R (W_R - W_R^*) - \lambda^* (W_R^* - W^*). \end{cases}$$

- (7) and 2nd invariant in (6) lead to:

$$h_L^* = \frac{(\phi h)^{HLL} + \alpha \phi_R (b_R - b_L)}{\alpha \phi_R + (1 - \alpha) \phi_L},$$

$$h_R^* = \frac{(\phi h)^{HLL} - (1 - \alpha) \phi_L (b_R - b_L)}{\alpha \phi_R + (1 - \alpha) \phi_L}.$$

- (5) and 3rd invariant (6) yield:

$$\lambda^* = \frac{\phi_L h_L (u_L - \lambda_L) + \phi_R h_R (u_R - \lambda_R)}{2(\phi h)^*} + \frac{\lambda_L \phi_L h_L^* + \lambda_R \phi_R h_R^*}{2(\phi h)^*}$$

- steady states at rest in (8) yield:

$$\Delta x \bar{S}_x = g \left(\frac{h_L h_R}{2} (\phi_R - \phi_L) \right) - g \left(\frac{\phi_L h_L + \phi_R h_R}{2} (b_R - b_L) \right)$$

$$\text{Semi-implicit scheme for (3): } (\phi h U)_j^{n+1} = \frac{(\phi h U)_j^{n+1/2}}{1 + \Delta t \left(\frac{\eta^2 g |U_j^n|}{(h_j^{n+1})^{4/3}} + \frac{1}{2} \frac{a C_d |U_j^n|}{\phi_j^2} \right)}$$

Numerical experiment

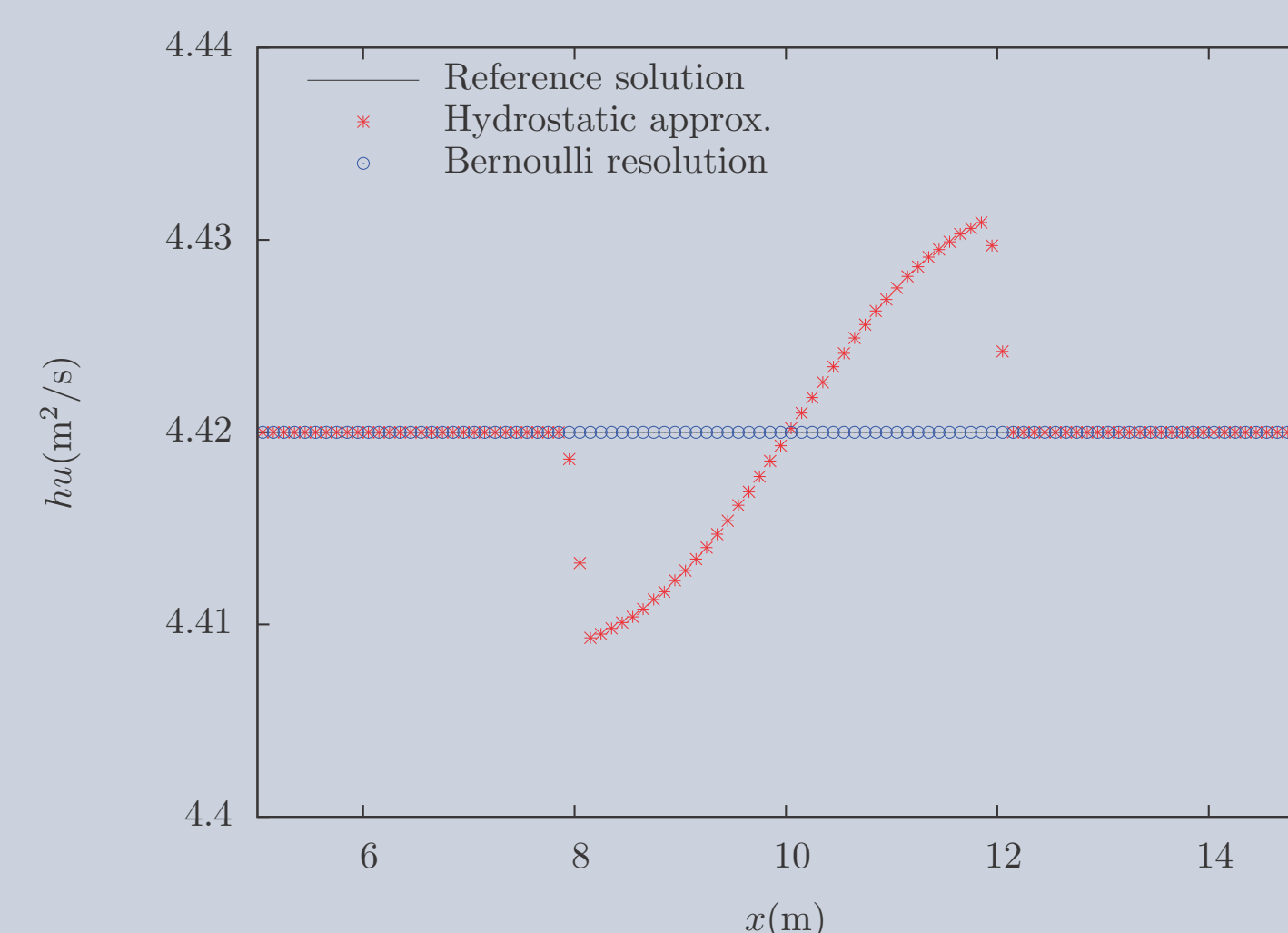


Figure: Steady sub-critical flow over a bump.

- ▶ well-known test case of SW model.
- ▶ Bernoulli relation in (6): $\frac{u_L^*{}^2}{2g} + h_L^* + b_L = \frac{u_R^*{}^2}{2g} + h_R^* + b_R.$
- ▶ hydrostatic approximation yields: $h_L^* + b_L = h_R^* + b_R.$
- ▶ as efficient as the PorAS scheme [2] for this type of regular solution.
- ▶ test case from [3], exact solution known.
- ▶ complex structure: 1-rarefaction wave, stationary discontinuity, 1-rarefaction wave then 2-shock wave.
- ▶ hydrostatic approximation: wrong solution unlike Bernoulli resolution.
- ▶ PorAs scheme can have difficulties to estimate shock waves speed.

- ▶ well-known test case of SW model.

- ▶ Bernoulli relation in (6):

$$\frac{u_L^*{}^2}{2g} + h_L^* + b_L = \frac{u_R^*{}^2}{2g} + h_R^* + b_R.$$

- ▶ hydrostatic approximation yields:

$$h_L^* + b_L = h_R^* + b_R.$$

- ▶ as efficient as the PorAS scheme [2] for this type of regular solution.

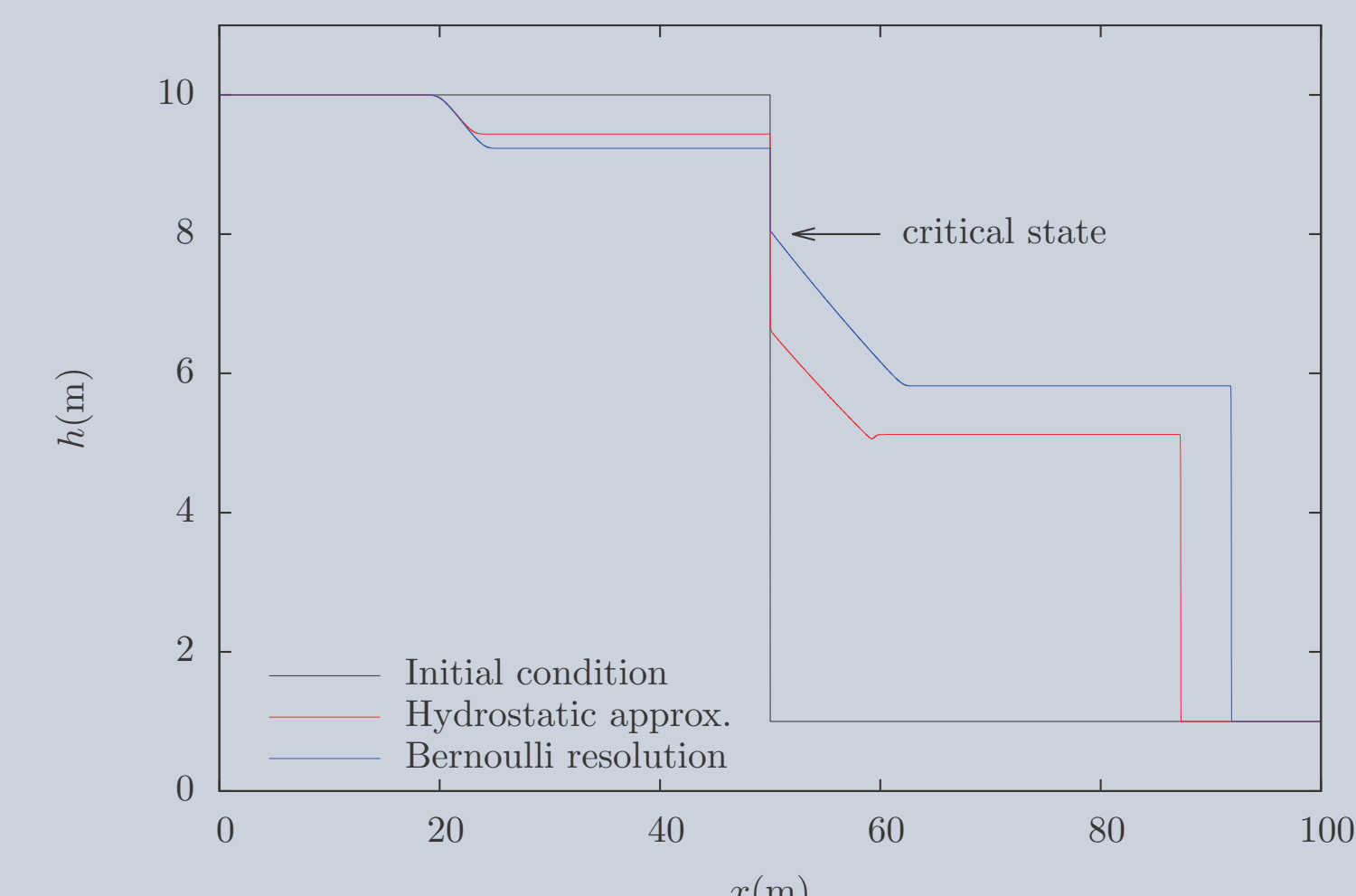


Figure: Dambreak with large porosity discontinuity.

Longitudinal transition from meadow to wood in a laboratory flume [4]:

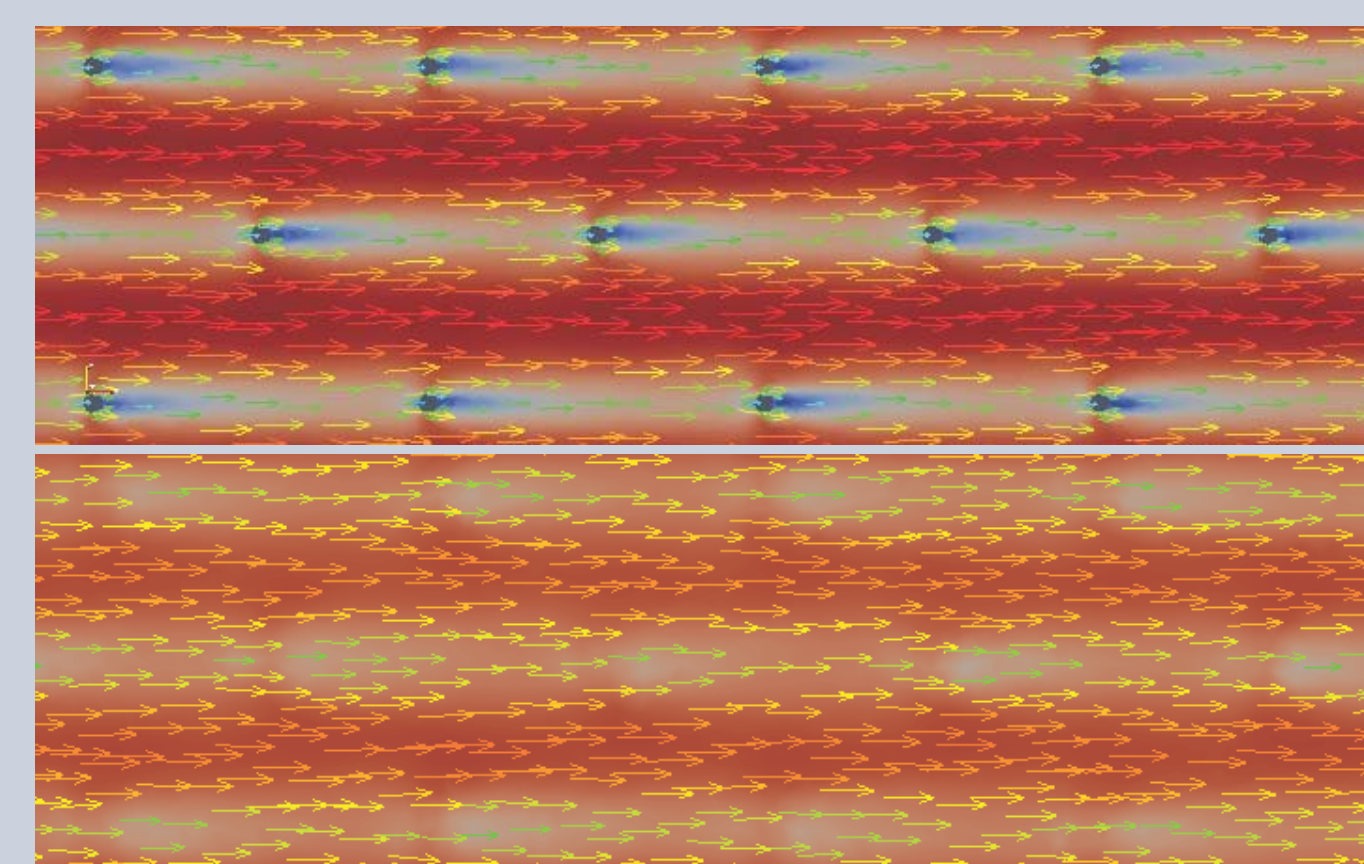


Figure: Velocity field and unit discharge in wood region: SW model (top) and SP model (bottom).

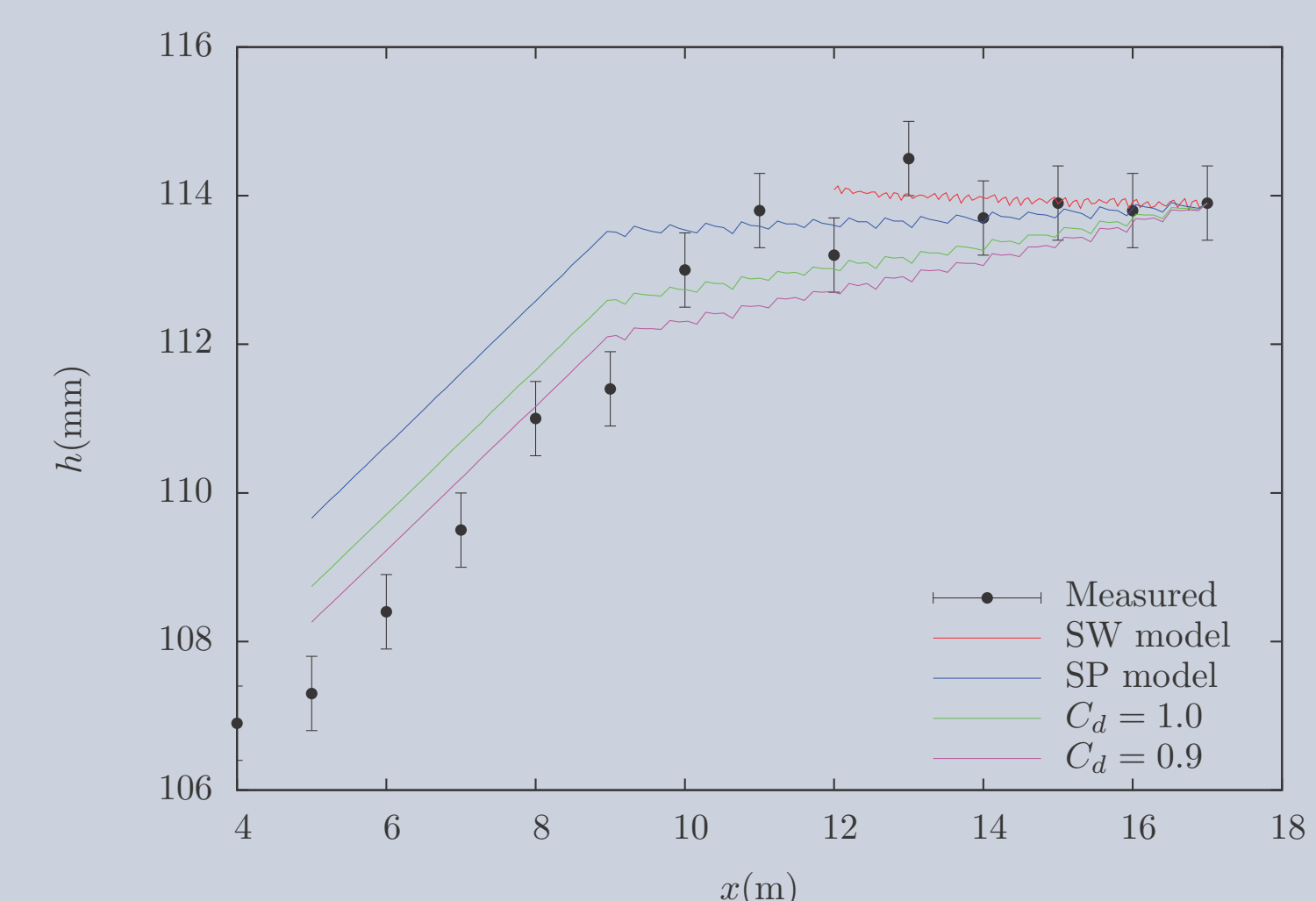


Figure: Water depth around the transition.

- ▶ emergent, rigid and circular vegetation distributed in staggered rows.
- ▶ expensive computation cost with SW.
- ▶ SP capture macroscopic behaviours.
- ▶ SP capture qualitative behaviour.
- ▶ agreement in wood region, $C_d = 1.2.$
- ▶ better compromise with $C_d = 1.$

Conclusions & Forthcoming Research

- ▶ augmented HLLC scheme well-balanced, positivity preserving and shock capturing.
- ▶ further test cases have to be implemented.

References

- [1] A. Defina, Water Resources Research **36**, 3251 (2000)
- [2] P. Finaud-Guyot, C. Delenne, J. Lhomme, V. Guinot, C. Llovel, Int. J. Numer. Meth. Fluids **62**, 1299 (2010)
- [3] V. Guinot, S. Soares-Frazão, Int. J. Numer. Meth. Fluids **50**, 309 (2006)
- [4] V. Dupuis, S. Proust, C. Berni, A. Paquier, Environmental Fluid Mechanics **16**, 1173 (2016)

Acknowledgements

Experimental data were provided by the FlowRes projet, supported by the French National Research Agency (ANR) under the grant No ANR14-CE003-0010. We acknowledge in particular V. Dupuis and S. Proust for their insightful comments.

Contact information

- ▶ M.-H. Le: minh-hoang.le@enpc.fr
- ▶ M. Oukacine: marina.oukacine@enpc.fr
- ▶ V. Dubos: dubos@ljl.math.upmc.fr
- ▶ N. Goutal: nicole.goutal@edf.fr